Membrane-Induced Folding of Cecropin A

Loraine Silvestro* and Paul H. Axelsen*†
Departments of *Pharmacology and †Medicine, Infectious Disease Section, and The Johnson Foundation for Molecular Biophysics, University of Pennsylvania School of Medicine, Philadelphia, Pennsylvania 19104-6084 USA

ABSTRACT Lipid membranes manifest a diverse array of surface forces that can fold and orient an approaching protein. To better understand these forces and their ability to influence protein function, we have used infrared spectroscopy with isotopic editing to characterize the 37-residue membrane-active antimicrobial polypeptide cecropin A as it approached, adsorbed onto, and finally penetrated various lipid membranes. Intermediate stages in this process were isolated for study by the use of internal reflection and Langmuir trough techniques. Results indicate that this peptide adopts well-ordered secondary structure while superficially adsorbed to a membrane surface. Its conformation is predominantly α-helical, although some β structure is likely to be present. The longitudinal axis of the helical structure, and the transverse axes of any β structure, are preferentially oriented parallel to the membrane surface. The peptide expands the membrane against pressure when it penetrates the membrane surface, but its structure and orientation do not change. These observations indicate that interactions between the peptide and deeper hydrophobic regions of the membrane provide energy to perform thermodynamic work, but separate and distinct interactions between the peptide and superficial components of the membrane are responsible for peptide folding. These results have broad implications for our understanding of the mechanism of action and the specificity of these antimicrobial peptides.

INTRODUCTION

Cecropin A is a linear 37-residue antimicrobial polypeptide produced by the cecropia moth as part of its defense against bacterial infection (Steiner et al., 1981; Hoffmann, 1995; Oren and Shai, 1998; Hancock and Chapple, 1999). There is a broad consensus that cecropin A and related peptides exert their antibacterial action on the plasma membrane, but its mechanism of action—and the way in which it recognizes and discriminates between bacterial and host cell membranes—remains unclear (Silvestro et al., 1997; Shai, 1999).

Cecropin A is unstructured in aqueous solution, but residues 5–21 and 24–37 have the potential to form amphiphilic α-helices in partially organic solvent (Steiner, 1982; Holak et al., 1988). Likewise, a cecropin A-melittin hybrid appears to increase its helicity upon partitioning from water to lipid vesicles (Mancheno et al., 1996). Structure-activity relationship studies have demonstrated that the presence and nature of several N-terminal residues are critical to the antibacterial activity of cecropin A against some organisms, but not against others (Andreu et al., 1983, 1985). Later studies of their bactericidal mechanism suggested that cecropins do not aggregate, but bind to negatively charged membrane lipids to form a closely packed layer (Steiner et al., 1988) or "carpet" of peptide (Pouny et al., 1992; Gazit et al., 1995), which renders the membranes permeable. Other studies of related peptides, however, have suggested that they do aggregate and then assume a transbilayer orientation in membranes (Mchaourab et al., 1993, 1994).

Cecropin A and related peptides form voltage-dependent ion channels with sequence-dependent conductivities (Christensen et al., 1988). In earlier studies we found the action of cecropin A on synthetic lipid vesicles to be concentration-dependent, with ion channels formed at low peptide/lipid ratios and "pores" large enough to pass various probe molecules formed at higher peptide/lipid ratios (Silvestro et al., 1997). The peptide was equally effective on anionic and neutral vesicles, even though anionic vesicles bound much larger amounts of peptide. We concluded that cecropin A adopts a fully active structure on both neutral and anionic membranes, but that anionic membranes bind a large amount of peptide that is inactive. The peptide was also effective on cholesterol-containing membranes, demonstrating that the presence or absence of cholesterol did not determine the specificity of peptide action. In the interim, we have sought to understand the structural basis for "membrane recognition" by this peptide, i.e., its mechanism of action and its ability to discriminate between bacterial and host cell membranes, by focusing on how and when this peptide folds into its final secondary and tertiary structure.

The process of membrane recognition may be divided into three stages: surface adsorption, monolayer penetration, and bilayer penetration. Folding of the peptide may occur at any stage, and the peptide may assume different folds at different stages. Valuable insights into membrane recognition may be gained by isolating and examining various intermediate states, irrespective of whether or not these states are visited when peptides normally interact with a membrane. For example, a diastereomeric analog of melittin has been used to model the "virtual" intermediate state in which the peptide is bound to the membrane, but not folded

Received for publication 10 March 2000 and in final form 15 June 2000.
Address reprint requests to Dr. Paul H. Axelsen, Depts. of Pharmacology and Medicine, Rm. 130/131, John Morgan Bldg., 3620 Hamilton Walk, University of Pennsylvania, Philadelphia, PA 19104-6084. Tel.: 215-898-9238; Fax: 215-573-2236; E-mail: axe@pharm.med.upenn.edu.

0006-3495/00/09/1465/13 $2.00

(Ladokhin and White, 1999). Because melittin and its analog appear to penetrate the membrane to the same degree (Oren and Shai, 1997), this analysis indicates that folding into an α-helix enhances partitioning of a peptide such as melittin into a membrane by 0.4 kcal/mol/residue.

In an effort to study other intermediate states relevant to membrane-induced peptide folding, we have coupled an infrared spectrometer to a Langmuir trough by means of an internal reflection crystal to perform polarized attenuated total internal reflection Fourier-transform infrared (PATIR-FTIR) spectroscopy (Axelsen et al., 1995a, b; Silvestro and Axelsen, 1998). This instrumentation provides quantitative information about the conformation and orientation of peptides on supported membranes under conditions in which it is possible to control membrane surface pressure. At normal surface pressures, penetration of the peptide into a monolayer is limited to half the distance that it could penetrate into a bilayer membrane. This isolates a monolayer-bound intermediate state for study. At high surface pressures (i.e., above the "critical insertion pressure") the peptide can adsorb to the surface, but it cannot penetrate into the hydrophobic region of a membrane. This isolates a superficially bound intermediate state for study.

We have characterized cecropin A in these two intermediate states using PATIR-FTIR spectroscopy and compared it to the corresponding data for cecropin A in several types of bilayer membranes and in aqueous and organic solution. Our results indicate that cecropin A assumes its final secondary structure and orientation while superficially adsorbed onto a membrane. Subsequent interactions with deeper hydrophobic regions provide energy for the peptide to perform thermodynamic work by expanding the membrane, but these interactions are not responsible for folding the peptide.

MATERIALS AND METHODS

Chemicals

Cecropin A and isotopically labeled variants were synthesized by Synpep Corporation (Sunnyvale, CA) according to the sequence KWKLFKKIEK VGQNIRDGII KAGPAVAVVG QATQIAK-$CONH_2$. Variant $CecA_{3-7}$ had ^{13}C labels in the carbonyl carbon of residues 3–7 and an ^{15}N label at residue 28. Variant $CecA_{26-30}$ had ^{13}C labels in the carbonyl carbon of residues 26–30 and an ^{15}N label at residue 5. All three peptides were purified locally by RP-HPLC and confirmed to have molecular masses of 4004 (unlabeled) and 4010 (labeled) by MALDI-TOF mass spectroscopy. Peptide stock solutions consisted of 1 mM peptide in D_2O buffer (30 mM Hepes, pD = 7.2). Dimyristoylphosphatidylcholine (DMPC) and dimyristoylphosphatidic acid (DMPA) were obtained from Avanti Polar Lipids (Alabaster, AL) and prepared as stock solutions of 1 mg/ml in hexane/ethanol at a ratio of 9:1. A solution containing DMPC and DMPA in a 4:1 molar ratio was prepared in the same solvent at 1 mg/ml. Contrad detergent and Hepes were obtained from Fisher Scientific (Fair Lawn, NJ). All water was glass-distilled. D_2O and deuterated 1,1,1,3,3,3-hexafluoro-2-propanol (*d*-HFP) were purchased from Cambridge Isotope Laboratories (Andover, MA). Phospholipid concentrations were determined by phosphate assay (Bartlett, 1959). Peptide concentrations were determined using a bicinchoninic acid assay (Pierce, Rockford, IL) with an albumin standard.

Transmission studies

Aliquots of cecropin A stock (20 μl at 10 μg/μl in D_2O) were spin-dried under vacuum and resuspended in 100 μl of either D_2O buffer (30 mM Hepes, pD = 7.2) or *d*-HFP/D_2O buffer (15% *d*-HFP, 85% D_2O, 30 mM Hepes, pD = 7.2) to yield 0.5 mM solutions. The pD of D_2O buffer solutions was measured by adding a correction factor of 0.4 to values obtained from a pH meter (Glasoe and Long, 1960). The addition of *d*-HFP to D_2O buffer lowered the pD to 6.9. For this reason, the pD was adjusted to 7.2 with 1 M NaOD before addition of cecropin A. Aliquots (20 μl) of buffer and these solutions were placed between CaF_2 windows with a 0.030 mm perfluorocarbon spacer.

Germanium crystal preparation

The internal reflection element for PATIR-FTIR studies was a 52 × 10 × 2 mm germanium crystal with 60° faceted apertures as described previously (Silvestro and Axelsen, 1999; Koppaka and Axelsen, submitted for publication). Crystals were cleaned by bath sonication for 10 min in 5% Contrad detergent, water ×2, methanol, and chloroform, followed by 15 min in a plasma cleaner (Harrick, Ossining, NY). The crystal surface was made hydrophobic by immersion into 5% octadecyltrichlorosilane in 50 ml hexadecane/carbon tetrachloride/chloroform (10:1.5:1) for 40 min while sonicating. The crystal was rinsed ×3 with ethanol, cured overnight at 90°C, and stored at room temperature until use.

Multibilayer studies

Aliquots of DMPC stock (20 μmol) were dried to a film under a stream of dry argon. The resultant film was resuspended in 1 ml D_2O buffer, sonicated for 10 min, and passed 11 times across a polycarbonate membrane (0.1 μm) using a miniextruder (Avanti Polar Lipids) to produce 100-nm diameter large unilamellar vesicles (LUV). The final lipid concentration was adjusted to 5 mM. The cecropin A stock solution was diluted to 0.25 mM. An aliquot of cecropin A (28 μl) was mixed with 70 μl of LUV and incubated for 15 min. The final concentrations of DMPC and cecropin A were 3.5 mM and 70 μM, respectively, for a lipid-to-peptide ratio of 50:1. An aliquot of the lipid/peptide mixture (5 μl) was applied onto one surface of a germanium crystal and dried under argon gas (1 h). The dried films were rehydrated with D_2O-saturated argon for 2 h at 25°C (Goormaghtigh et al., 1994).

Bilayer studies

Bilayers were prepared by the direct fusion of small unilammelar vesicles (SUV) to a clean germanium crystal (Brian and McConnell, 1984; Kalb et al., 1992). The SUV suspension (1 mM DMPC in D_2O buffer, 30 mM Hepes, 150 mM NaCl, pD = 7.2) was created by sonication of a lipid solution until clear (300W bath sonicator, Laboratory Supplies, Inc., Hicksville, NY). A crystal cleaned as above and left unsilanized was placed in a flow cell with a 50-μl compartment adjacent to the surfaces of a germanium crystal. Two hours after applying the SUV suspension to the crystal, the compartments were rinsed with calcium-containing buffer (1 mM $CaCl_2$, 30 mM Hepes), resulting in spontaneous fusion of the vesicles into bilayers (as evidenced by a marked decline in dichroic ratios for methylene stretching vibrations). Lipid films were washed with a 50× volume excess of 30 mM Hepes D_2O buffer (pD = 7.2) to remove unfused vesicles and residual calcium. Infrared spectra were collected after bilayers were incubated with a 5 μM cecropin A solution for 40 min.

Monolayer studies

Monolayer membranes were prepared by applying a solution of DMPC or DMPC/DMPA in hexane/ethanol onto the surface of D_2O buffer (6 ml) in

a Langmuir trough. The trough was housed in a chamber filled with D_2O-saturated argon to eliminate hydrogen/deuterium exchange in the samples. Surface pressure measurements were measured with a Wilhelmy wire (Momsen et al., 1990). The membrane was compressed to a selected pressure after allowing the hexane/ethanol to evaporate for 15 min. Monolayer membranes were applied to the bottom surface of a silane-treated germanium crystal by application of the crystal flat onto the air-water interface. Cecropin A (40 μg in 40 μl) was injected beneath the membrane surface into the continuously stirred buffer subphase to yield a final subphase peptide concentration of 1.7 μM.

Insertion pressure measurement

The critical insertion pressure (CIP) for cecropin A into a DMPC monolayer was determined using a du Noüy ring tensiometer (Adamson, 1990). Measurements of the increase in membrane pressure with addition of cecropin A were taken with a Fisher Autotensiomat equipped with a 6-cm-circumference wire platinum ring with wire thickness 1.1 mm. The balance was calibrated with a 1 g mass and checked against water (73 dyne/cm). An aliquot of DMPC (4–8 μl of 1 mg/ml in hexane/ethanol) stock solution was applied to the surface of 6 ml of D_2O buffer, and the solvent evaporated for 15 min. The membrane pressure was recorded before and 15 min after the injection of cecropin A (40 μg in 40 μl, 0.25 mM stock) into the buffer.

Internal reflection IR spectroscopy

PATIR-FTIR spectroscopy was performed with a BioRad FTS-60A spectrometer, equipped with an aluminum wire grid polarizer and a liquid nitrogen-cooled MCT detector, in a configuration as described (Axelsen et al., 1995a,b; Wimley et al., 1998) and modified (Silvestro and Axelsen, 1999). Spectra were collected at room temperature, a scan speed of 20 kHz, a resolution of 2 cm^{-1}, with triangular apodization and one level of zero filling. The angle of incidence between the IR beam and the crystal surface was 30°, for which the two-phase approximation yields an isotropic dichroic ratio of 2.33 (Axelsen and Citra, 1997; Koppaka and Axelsen, submitted for publication). Spectra of monolayer and bilayer membranes were the result of 1024 co-added interferograms for both parallel and perpendicular polarized light. Transmission and multibilayer spectra were obtained from 512 co-added interferograms.

Linked analysis

Spectra were fit using the program "Irfit" to perform quantitative analysis of absorption bands (Silvestro and Axelsen, 1999). In Irfit, each spectrum is fit with one straight and level baseline, and one or more bands. Each band is specified by four parameters: frequency, amplitude, full-width at half-maximum (FWHM), and shape (% Gaussian, remainder = Lorentzian); initial values for each parameter must be selected. The program then adjusts the values of these parameters by means of the downhill simplex method (Press et al., 1986) to achieve minimum least-squares residuals. No smoothing, water vapor subtraction, or deconvolution was performed on any of the spectra. Each spectrum was fit with the minimum number of bands sufficient to meet three criteria: 1) narrow uncorrelated residual amplitudes (FWHM $<$ 10 cm^{-1}), 2) a ratio of spectral amplitudes to residual amplitudes that corresponded to the apparent signal-to-noise ratio of the original spectra, and 3) reduction of the χ^2 gradient to within one order of magnitude of single-precision arithmetic.

Order parameters

From the polarized absorption spectra, dichroic ratios $R_z = \int A_\parallel / \int A_\perp$ were evaluated using integrated areas of characteristic absorption bands, $\int A$, as described previously (Silvestro and Axelsen, 1999). Dichroic ratios were converted to order parameters, $S(R_z)$, according to Eq. 1

$$S(R_z) = \frac{\langle E_x^2\rangle - R_z\langle E_y^2\rangle + \langle E_z^2\rangle}{\langle E_x^2\rangle - R_z\langle E_y^2\rangle - 2\langle E_z^2\rangle} \tag{1}$$

$$= \langle P_2(\cos\theta)\rangle\langle P_2(\cos\gamma)\rangle\langle P_2(\cos\xi)\rangle \tag{2}$$

$$= S_\theta S_\gamma S_\xi \tag{3}$$

using the two-phase approximation to calculate the mean electric field amplitude components $\langle E_x^2\rangle = 2.822$, $\langle E_y^2\rangle = 3.367$, and $\langle E_z^2\rangle = 5.000$ (Citra and Axelsen, 1996; Axelsen and Citra, 1997). Only this approximation was used because of recent evidence corroborating its validity for systems of this type (Koppaka and Axelsen, submitted for publication). Angle brackets indicate mean values, $P_2(x) = (3x^2 - 1)/2$ is the second-order Legendre polynomial which relates to order parameters according to $S_x = \langle P_2(\cos x)\rangle$, θ is the angle between the molecular axis and the vibrational transition moment, γ is the angle between the molecular axis and the membrane normal, and ξ is the angle representing the orientation of the monolayer surface with respect to the crystal surface (the mosaic spread) (Axelsen et al., 1995b). An order parameter of 1.0 indicates a uniform orientation perpendicular to the membrane surface, while a value of -0.5 indicates a uniform orientation parallel to the membrane. An order parameter of 0.0 may indicate either a uniform orientation at the magic angle (54.7° relative to the membrane normal), complete disorder as in an isotropic system, or any other orientation distribution for which $\langle \cos^2 x\rangle = 1/3$. For an isotropic sample and the experimental configuration used in this work, the isotropic dichroic ratio is

$$R_{ISO} = \frac{\langle E_x^2\rangle + \langle E_z^2\rangle}{\langle E_y^2\rangle} = 2.33. \tag{4}$$

The total absorption, corrected for differences in intensity for the two polarizations, was calculated from

$$k = \frac{A_\parallel}{\langle E_z^2\rangle} + \frac{A_\perp}{\langle E_y^2\rangle}\cdot\left(2 - \frac{\langle E_x^2\rangle}{\langle E_z^2\rangle}\right) \tag{5}$$

(see Appendix and Marsh, 1999).

RESULTS

Transmission studies

Transmission spectra of cecropin A were recorded in a D_2O buffer and in a D_2O buffer with 15% deutero-hexafluoropropanol (*d*-HFP/D_2O) (Fig. 1, type TR). The absorbance maximum of the amide I′ for cecropin A was 1647 cm^{-1} in D_2O buffer and it decreased to 1643 cm^{-1} in *d*-HFP/D_2O (Fig. 2). Amide I′ absorbance narrowed slightly (from 50 cm^{-1} to 43 cm^{-1} at half-maximum) and became more symmetric in *d*-HFP/D_2O, suggesting more uniformity in backbone secondary structure. These results correlate to circular dichroism (Steiner, 1982) and NMR (Holak et al., 1988) studies performed earlier under the same conditions. The latter demonstrated that cecropin A folds into a pair of α-helical segments connected and terminated by short random segments in *d*-HFP/D_2O, while both techniques showed that essentially all secondary structure is lost when the concentration of HFP is reduced from 15 to 0%. The

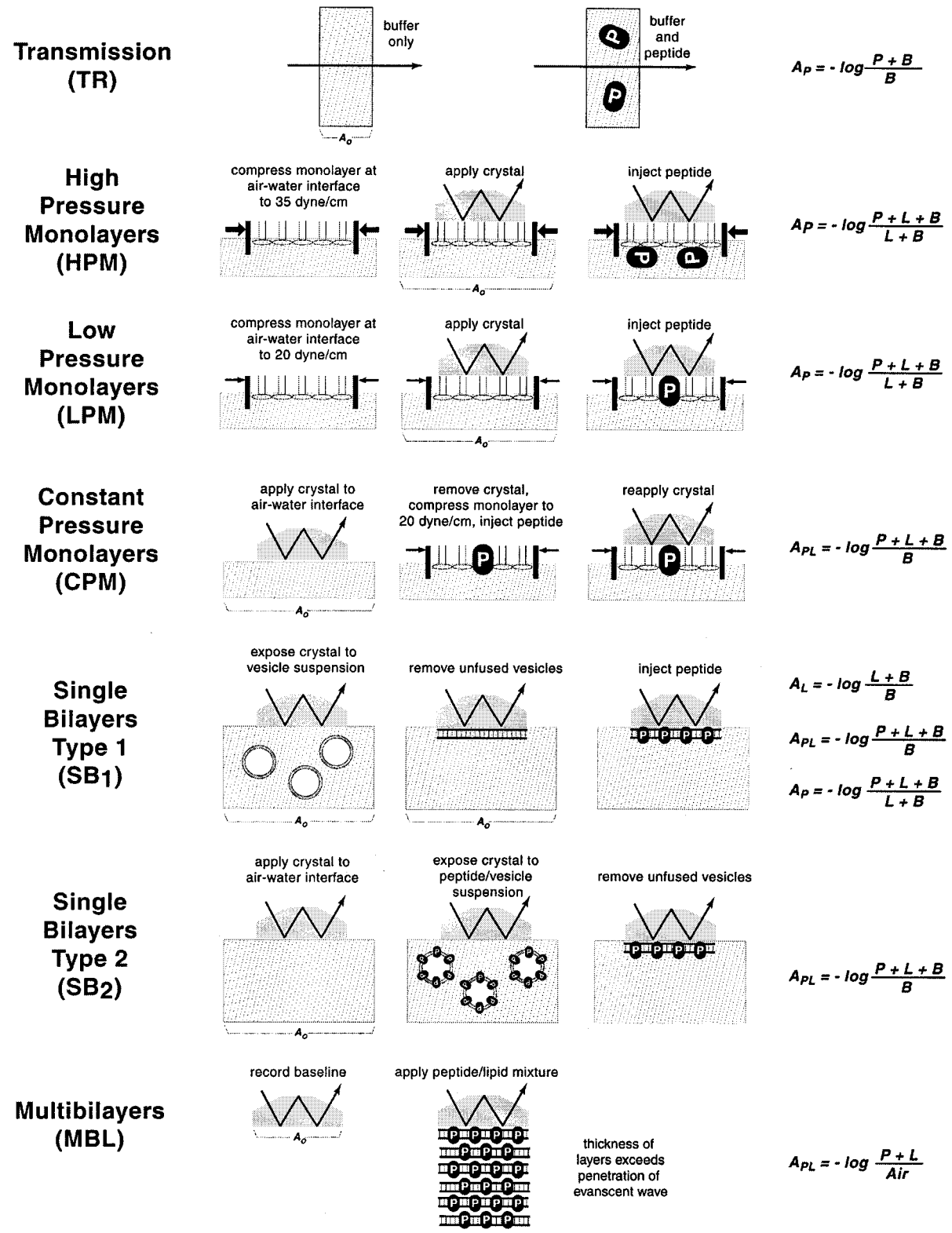

FIGURE 1 A schematic description of key steps in each type of experiment. Hatched regions in TR experiments represent aqueous buffer between CaF_2 windows; in all other experiment types they represent aqueous buffer in a Langmuir trough. The shaded polygon with a segmented arrow is an internal reflection crystal with an internally reflecting IR beam, and objects marked P represent peptide. Circular objects in SB_1 experiments are phospholipid vesicles; in SB_2 experiments they have been pre-reacted with peptide. The spectral information derived from each experiment is indicated in a column on the right side: A_P is the absorption due to peptide P, A_L is the absorption due to lipid L, and A_{PL} is the absorption due to both protein and lipid. A spectral

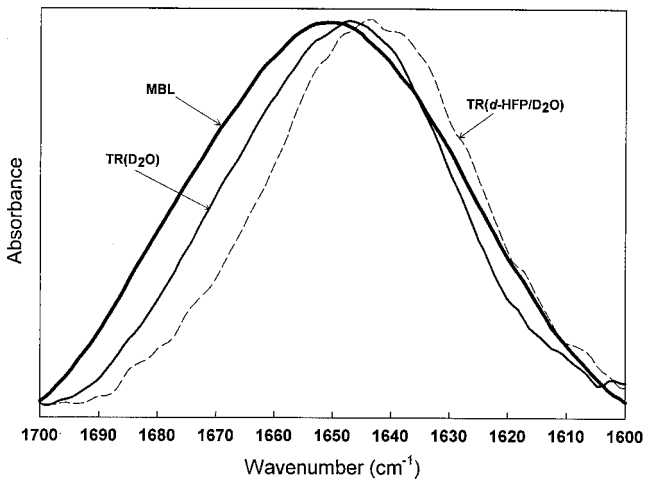

FIGURE 2 Spectra from type TR experiments for cecropin A in D_2O and *d*-HFP/D_2O, compared to a spectrum from an MBL experiment for cecropin A in DMPC. Spectra have been normalized to equivalent maximum amplitude, but have not been smoothed, deconvolved, corrected for water vapor, or adjusted for a non-level baseline. The spectral differences cannot be explained by distortion due to anomalous dispersion in the internal reflection spectra because the absorption coefficients in these spectra are small enough that "true" extinction coefficient spectra obtained by iterative correction procedures involving the Kramers-Kronig transform (Ohta and Ishida, 1988; Huang and Urban, 1992; Yamamoto and Ishida, 1994; Urban, 1996) are indistinguishable from the original absorption spectrum. Furthermore, anomalous dispersion would cause distortion of the MBL spectrum toward lower frequencies, not higher frequencies as seen here.

transmission IR spectra collected under these conditions, therefore, constitute reference spectra for unstructured peptide and for the α-helical conformation. The latter is especially valuable because α-helical conformation is frequently and inconsistently "assigned" to absorption bands as high as 1655 cm^{-1}. (NOTE: we follow the convention that amide I′ refers to amide I absorption recorded in D_2O.)

Multibilayer studies

Internal reflection infrared spectra of cecropin A were recorded in supported planar multilammelar DMPC membranes (multibilayers) to compare the aforementioned spectra obtained in solution with spectra obtained in a phospholipid environment. Multibilayer experiments were performed in four steps: first, a background spectrum was recorded from a dry silanized germanium crystal. Second, an aqueous suspension of cecropin A and lipid vesicles was deposited on the crystal. Third, after the water had evaporated, D_2O-saturated argon was circulated around the crystal for 2 h. Finally, a sample spectrum was recorded against the background collected in step one (Fig. 1, type MBL).

In MBL experiments, amide I′ was maximal at 1651 cm^{-1} and considerably broader at 65 cm^{-1} than either of the spectra obtained via transmission (Fig. 2). The lipid acyl chains were well ordered with $S(R_z) = -0.32 \pm 0.05$ for the symmetric methylene stretching mode at 2851 cm^{-1}. The overall dichroic ratio for amide I′ in MBL experiments was 1.59, corresponding to an order parameter of $S(R_Z) = -0.20 \pm 0.04$. Given that $S_\theta \approx 0.53$ for an α-helix (Axelsen et al., 1995b), and that there are absolute limits on horizontal order ($S_\gamma \geq -0.50$) and mosaic spread ($S_\xi \leq 1.00$), we obtain a lower limit for the orientational order of an α-helix of $S(R_Z) \geq -0.27$ from Eq. 3. Thus, even though the conformation of cecropin A in multibilayers is not known, nor is it clear from these spectra, the overall orientational order of its peptide groups is close to the theoretical limit for a perfectly horizontal α-helix (Axelsen et al., 1995b). This is consistent with ^{15}N-NMR studies in the same type of preparation (Marassi et al., 1999).

Single bilayer studies

Infrared spectra of cecropin A in supported single DMPC bilayer membranes were recorded to characterize the peptide in a fully hydrated bilayer membrane. These experiments were performed in six steps. First, a background spectrum was collected from an unsilanized (hydrophilic) germanium crystal that was superfused with buffer in a flow cell. Second, bilayer membranes were applied to the crystal surface by introducing a lipid vesicle suspension into the flow cell. Third, after allowing time for self-assembly of the membrane, the flow cell was perfused with buffer until the magnitude and dichroic ratio of the methylene stretching bands stabilized. Fourth, a second background spectrum was collected. Fifth, the peptide was introduced into the flow cell for 10–15 min and then washed out. Finally, the sample spectrum was recorded against the background from step four (Fig. 1, type SB_1).

In spectra recorded after step 3, the membrane lipids are well ordered with $S(R_Z) = -0.37 \pm 0.07$ for the symmetric methylene stretching mode at 2851 cm^{-1}. In spectra recorded after the final step, the shape of amide I′ was similar to that observed in *d*-HFP/D_2O except for increased absorption between 1600 and 1620 cm^{-1} and between 1655 and 1680 cm^{-1} (Fig. 3). There were absorbance changes evident in the methylene stretching regions of the spectrum (Silves-

signal from the aqueous buffer *B* is present in all spectra except MBL. For example, P + L + B in a numerator indicates that peptide, lipid, and buffer signals are present in a sample spectrum; L + B in a denominator indicates that lipid and buffer signals were recorded in the baseline spectrum, and the resulting absorption spectrum will be A_P. The step at which the baseline spectrum is collected in each experiment is indicated by A_0. In SB_1 experiments, the baseline and sample spectra may each be recorded at two different steps, yielding three different types of spectra as indicated.

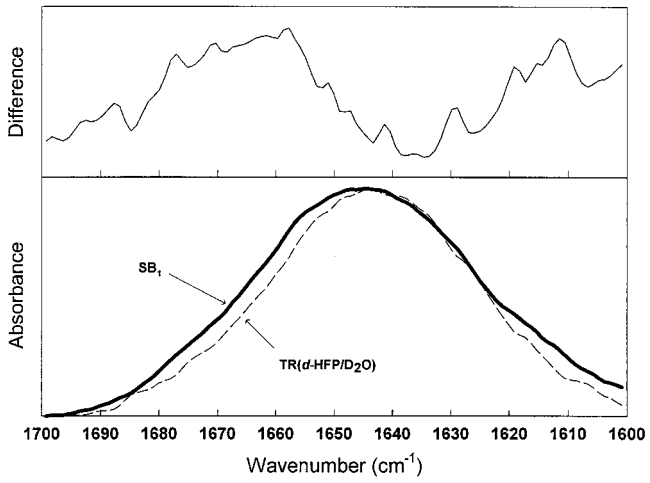

FIGURE 3 Spectra from an SB_1 experiment compared to a type TR experiment for cecropin A in *d*-HFP/D_2O. The SB_1 spectrum is the average of three spectra collected on three different days, and both spectra have been normalized to equivalent maximum amplitude, but neither one has been smoothed, deconvolved, corrected for water vapor, or adjusted for a non-level baseline. As with the MBL spectrum in Fig. 2, the correction due to anomalous dispersion in SB_1 spectra is negligible due to their low absorption amplitudes.

tro and Axelsen, 1998), suggesting that peptide penetration displaced lipids from the surface, or at least altered their orientation in the bilayer.

Because the presence of a solid support adjacent to the bilayer may not permit the peptide to insert normally, an experiment was performed in which the peptide was added to the lipid vesicle suspension before applying the membranes to the support (Fig. 1, type SB_2). The amide I′ spectra from this experiment were indistinguishable from those in which peptide was added to the subphase after applying the membranes to the support.

There is a clear difference between the spectra obtained from these bilayers and those obtained from multibilayers (Figs. 2 and 3). The differences may be due to several factors, including the relative paucity of water in multibilayer preparations (Wiener and White, 1992; White and Wiener, 1995). Without enough water to separate the bilayers in a multibilayer preparation, the presence of a peptide is likely to disrupt the packing of bilayers against each other, and it will most likely interact with more than one bilayer simultaneously (Silvestro and Axelsen, 1998).

Critical insertion pressure

The critical insertion pressure of cecropin A in supported DMPC and DMPC/DMPA monolayer membranes appeared to lie between 25 and 30 dyne/cm. At pressures below this range, the injection of peptide into the subphase increased monolayer surface pressure. Conversely, the injection of peptide into the subphase at surface pressures above this range had no effect on monolayer surface pressure. Ring tensiometry corroborated these results for DMPC, yielding a critical insertion pressure of 28 $\pm$ 2 dyne/cm.

Monolayer studies

Infrared spectra of cecropin A in monolayer membranes were recorded to characterize the peptide at two different intermediate stages in its association with a bilayer membrane. High pressure monolayer (HPM) experiments were performed above the critical insertion pressure at 35 dyne/cm. This isolates the peptide at a stage in which it is superficially adsorbed and unable to penetrate the membrane. Low pressure monolayer (LPM) experiments were performed below the critical insertion pressure at 20 dyne/cm. This isolates the peptide at a monolayer-inserted stage in which its penetration is limited to half the distance it might penetrate into a bilayer. HPM and LPM experiments were performed in four steps. First, a monolayer at known pressure was applied to one surface of the germanium crystal using the Langmuir trough. Second, a background spectrum was recorded. Third, peptide was introduced into the trough subphase. Finally, the sample spectrum was recorded against the background collected in step two.

LPM and HPM experiments with DMPC all featured a single broad amide I′ absorbance virtually identical in shape and position to that obtained from SB_1 experiments. LPM experiments with DMPC/DMPA were also performed and similar results were obtained (discussed further below). No changes in absorbance of methylene stretching modes in the lipids were detected in LPM or HPM experiments.

In LPM and HPM experiments, the peptide was injected into the subphase buffer after the monolayer membrane was applied to the crystal, and after a background spectrum was recorded. In this type of experiment it was relatively easy to keep the spectral baseline straight and level because the only manipulation performed between the collection of background and sample spectra was the injection of peptide into the subphase. However, we could not measure surface pressure within the supported portion of the monolayer, and phospholipid molecules in the supported portion were not in equilibrium with those elsewhere in the trough at the air-water interface. Insertion of just a few peptides into a low pressure membrane, therefore, had the potential to dramatically increase local surface pressure.

For this reason, we examined DMPC membranes that were allowed to expand at a constant pressure after peptide was introduced into the subphase (Fig. 1, type CPM). This type of experiment involved seven steps, and was more complicated than LPM or HPM experiments. First, a background spectrum was recorded with the internal reflection crystal in direct contact with buffer. Second, the crystal was removed from the buffer and dried. Third, a monolayer was prepared on the buffer surface and compressed to 20 dyne/cm. Fourth, peptide was introduced into the subphase and

the membrane was allowed to expand at constant pressure as the peptide inserts. Fifth, membrane expansion was halted after several minutes by replacing the subphase with peptide-free buffer. Sixth, the crystal was re-applied to the air-water interface where a peptide/lipid monolayer has formed. Finally, a sample spectrum was collected against the background obtained in step one.

There are three key findings from CPM experiments pertaining specifically to the lipid phase. First, the injection of peptide into the subphase during a CPM experiment causes membrane expansion to occur against a surface pressure of 20 dyne/cm. This indicates that the peptide performs thermodynamic work on the membrane. Second, the replacement of the subphase with peptide-free buffer halts, but does not reverse, this expansion. This indicates that the off-rate for peptide penetration is considerably slower than the on-rate, consistent with a strong thermodynamic driving force for peptide penetration. Third, the phospholipid acyl chains are highly ordered with $S(R_Z) = -0.33 \pm 0.02$ for the symmetric methylene stretching mode at 2853 cm^{-1}. This is the same degree of order seen in the absence of peptide (Axelsen et al., 1995a,b) and it indicates that the peptides have penetrated deep into the hydrophobic acyl chain region of the membrane. If the peptide did not interact directly with the acyl chains, the new space between the acyl chains resulting from membrane expansion would have to be filled by tilting and disordering of the acyl chains. As mentioned above, this is readily seen in SB_1 experiments (Silvestro and Axelsen, 1998). In contrast to CPM experiments, interactions with the crystal support prevent the lipid phase from fully relaxing upon peptide penetration in SB_1 experiments.

The amide I′ spectra from CPM experiments are virtually identical to those obtained from SB_1 experiments (Fig. 4). To assign spectral components to specific segments within cecropin A, an isotopic editing strategy was used in which the peptide was synthesized with ^{13}C in the carbonyl carbon of either residues 3–7 ($CecA_{3-7}$), or residues 26–30 ($CecA_{26-30}$). Compared to spectra from unlabeled peptide, the labels shift a significant component of amide I′ absorption to lower frequencies (Fig. 5). The shapes of amide I′ for $CecA_{3-7}$ and $CecA_{26-30}$ in CPM experiments also differ from each other. A quantitative analysis of CPM spectra follows.

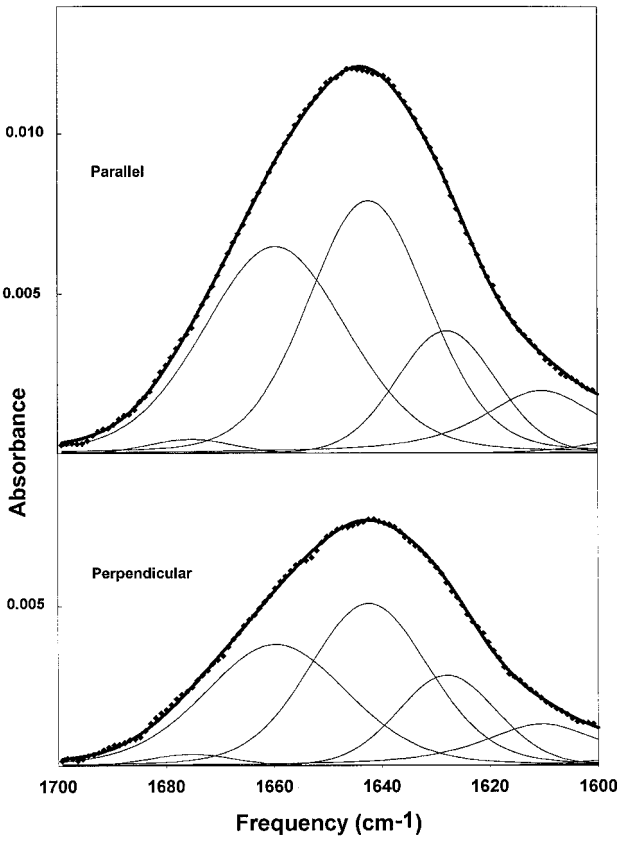

FIGURE 4 IRfit analysis of spectra from type CPM experiments, 1700–1600 cm^{-1}. The spectra in both panels represent the average of three spectra collected on three different days, and are unprocessed except for subtraction of a straight and level baseline by IRfit. Averaged raw data are represented by filled symbols. The thin lines represent fitted components, for which parameters may be found in Table 1. The bold line generally running through the data represents the sum of the fitted components.

IRfit analysis

The spectra recorded in some of the experiments described above were subjected to linked simultaneous analysis using IRfit, a procedure that attempts to find the fewest number of components that can simultaneously and completely describe a set of related spectra. Each spectrum in a set of n spectra is fit with a single straight and level baseline, and each of m components is described by four parameters: frequency, amplitude, width, and shape. Each component is constrained to have the same frequency, width, and shape in each of the spectra being fitted (i.e., three of the four parameters are "linked" across the whole set of spectra); only the component amplitudes are allowed to vary independently between spectra. Thus, the number of independent fitting parameters (n baselines, $3 \cdot m$ linked parameters, plus $n \cdot m$ independent amplitudes) is less than conventional band-fitting approaches (n baselines plus $4 \cdot n \cdot m$ independent parameters). Beyond eliminating $(n - 1) \cdot (3 \cdot m)$ fitting parameters, this approach facilitates quantitative comparisons of different spectra and the calculation of dichroic ratios. A detailed description of the application and advantages of IRfit has been published elsewhere (Silvestro and Axelsen, 1999).

Two sets of spectra were subjected to IRfit analysis. The first set consisted of six spectra each (three parallel and three perpendicularly polarized) from five different experiments (30 spectra): SB_1, LPM with DPMC, LPM with DMPC/DMPA, HPM with DMPC, and CPM with DMPC. For the region between 1600 and 1700 cm^{-1}, IRfit recovers

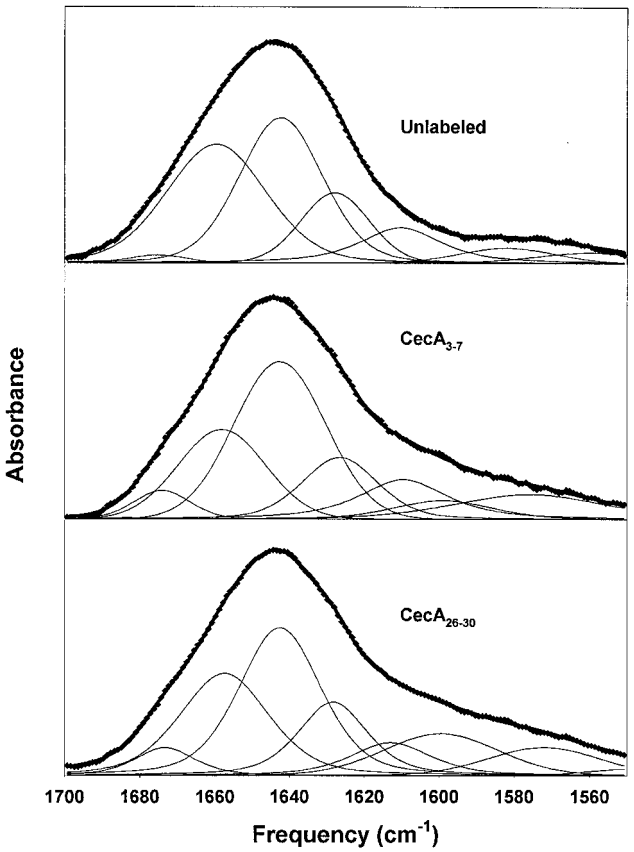

FIGURE 5 IRfit analysis of spectra from type CPM experiments, 1700–1550 cm^{-1}. Results from unlabeled peptide, and peptide labeled with ^{13}C in residues 3–7 and in residues 26–30 are compared. Symbols and lines are as for Fig. 4. Parameters for the fitted components are provided in Table 2.

major components at 1612.0, 1628.0, 1642.3, and 1659.0 cm^{-1} (Fig. 4 and Table 1). The most striking finding among these results is their similarity across different experiment types. All spectra in all five experiments are well-described by nearly identical parameters, reflecting similar total absorptions among the different experiments for each of the three different components, and similar dichroic ratios. The isotropic dichroic ratio for this apparatus is 2.33, so that ratios above this value indicate preferential orientation perpendicular to the membrane surface, and ratios less than this indicate preferential orientation parallel to the membrane surface. Overall, the dichroic ratios indicate a strong trend for the orientation of amide I′ transition moments to be in the plane of the membrane, i.e., $R_Z < 2.33$. We conclude that cecropin A adopts the same well-ordered and horizontally oriented secondary structure in all monolayer and bilayer experiments.

A minor exception to an otherwise narrow range of dichroic ratios is seen in LPM experiments with DMPC and DMPC/DMPA membranes (Table 1). We suspect that dichroic ratios for these experiments tend to be higher (i.e., less well-ordered) because lipid molecules in the supported portion of a low pressure monolayer are not in equilibrium with lipid molecules at the air-water interface in an LPM experiment. Consequently, the peptide will increase local surface pressure when it inserts into a supported monolayer, and inconstant pressure probably leads to a relatively disordered final state.

The second set of spectra subjected to IRfit analysis included six spectra each from CPM experiments with unlabeled cecropin A and isotopically labeled cecropin A: $CecA_{3-7}$ and $CecA_{26-30}$ (18 spectra). As in the first set, each set of six included three parallel and three perpendicularly polarized spectra. The only difference in the fitting procedure used was that the fit was performed over the region from 1700 to 1550 cm^{-1}. A simultaneous fit of all 18 spectra, however, was of only mediocre statistical quality. Therefore, spectra from the three different types of experiments were "unlinked" from each other, and further optimization of the fit was performed starting with the parameters obtained from the simultaneous fit. Even though the value of the fitting parameters only changed by rather small amounts (Table 2), this dramatically improved the statistical quality of the fits (Fig. 5). It should also be noted that fitting the CPM experiments independently and over a wider range of frequencies (1700–1550 cm^{-1}) yielded results that were not substantially different from a fit over 1700–1600 cm^{-1} (Tables 1 and 2).

To a first approximation, and neglecting changes in extinction coefficients, one would expect labeling of 5/37 peptide bonds to red-shift 13–14% of the absorption by ~37–40 cm^{-1} (Tadesse et al., 1991). As seen in Table 2, labeling of residues 3–7 in $CecA_{3-7}$ did shift 15% of the total absorbance away from ~1659 cm^{-1}. A corresponding increase was seen at ~1609 and ~1575 cm^{-1}. The shift caused an increase in the dichroic ratio at ~1659 cm^{-1} and decreased at the lower frequencies. Given the limiting order parameter for a perfectly horizontal α-helix, $S(R_Z) \geq -0.265$ (vide supra), we obtain $R_Z \geq 1.39$ from Eq. 1. Therefore, the dichroic ratios found for the low-frequency components ($R_Z = 1.21, 1.29$) are lower than is seemingly possible from an α-helix and not isotropically oriented, as one would expect from "frayed" ends of a helix. This suggests that residues 3–7 have a highly ordered but nonhelical structure, and it is intriguing in light of earlier structure-activity relationships demonstrating the functional importance of residues near the amino terminus (Andreu et al., 1983, 1985; Steiner et al., 1988).

Labeling of residues 26–30 in the $CecA_{26-30}$ peptide shifted 10% of the total absorbance away from ~1659 cm^{-1}, with corresponding increases at 1572 and 1599 cm^{-1}. In this case, however, the shift caused a decrease in the dichroic ratio at 1659 cm^{-1} as well as at the lower frequencies. This suggests that residues 26–30 have a dichroic ratio between the values of 1.69 and 2.02. Because these ratios are greater than 1.39 (the limiting value for an α-helix, see above), and less than 2.33 (the isotropic ratio),

TABLE 1 IRfit analysis of spectra from unlabeled peptides

Frequency	1612.0	1628.0	1642.3	1659.0	1675.1
Width (FWHM)	21.2	20.1	26.3	32.0	14.2
Shape (% Gauss)	45.3	50.0	66.2	57.1	50.0
k value					
SB_1-DMPC	9 (<1)	16 (<1)	40 (<1)	34 (<1)	1 (<1)
LPM-DMPC	5 (1)	17 (1)	43 (2)	34 (3)	2 (<1)
LPM-DMPC/DMPA	4 (1)	15 (1)	40 (2)	38 (1)	3 (1)
CPM-DMPC	7 (1)	16 (2)	39 (2)	36 (2)	1 (1)
HPM-DMPC	4 (2)	17 (3)	40 (2)	36 (2)	3 (1)
R_Z value					
SB_1-DMPC	1.34 (0.11)	1.31 (0.04)	1.39 (0.06)	1.68 (0.09)	0.51 (0.19)
LPM-DMPC	2.32 (0.40)	1.76 (0.12)	1.90 (0.03)	2.78 (0.36)	3.48 (0.88)
LPM-DMPC/DMPA	2.54 (0.88)	1.52 (0.08)	1.68 (0.01)	2.26 (0.18)	2.76 (0.57)
CPM-DMPC	1.58 (0.21)	1.40 (0.18)	1.56 (0.03)	1.70 (0.07)	1.70 (0.65)
HPM-DMPC	0.96 (0.60)	1.27 (0.10)	1.46 (0.05)	2.00 (0.05)	2.36 (0.30)

Spectra were fitted with IRfit over the frequency range 1700–1600 cm^{-1}. Total absorbance, *k*, is a percentage of total absorbance, and is calculated according to Eq. 5. The isotropic ratio (R_{ISO}) = 2.33 according to Eq. 4. Values of $R_Z > R_{ISO}$ indicate preferential orientation perpendicular to the membrane surface; values of $R_Z < R_{ISO}$ indicate preferential orientation parallel to the membrane. $R_Z = 0.84$ is the minimum possible dichroic ratio, corresponding to perfectly parallel orientation.
Values in parentheses represent the mean deviations of each result from an IRfit analysis of 30 spectra.

these ratios are consistent with a horizontally oriented α-helix. The substitution of ^{13}C for ^{12}C should only red-shift IR absorption by 37 cm^{-1} (Tadesse et al., 1991), but the data suggest that shifts of 47–100 cm^{-1} have occurred. Furthermore, both of the labeled peptides exhibit a paradoxically increased absorbance at high frequencies, ~1673–1674 cm^{-1}. We suspect these anomalies arise because isotopic substitution has uncoupled vibrational modes that would otherwise be subject to mechanical and dipolar (i.e., "vibronic") coupling, and that this uncoupling has caused complex shifts in the absorption frequencies of the remaining unlabeled segments (Decatur and Antonic, 1999).

DISCUSSION

Principal conclusions and assumptions

These studies provide information about the conformation and orientation of this peptide in diverse physical circumstances: lipid-free aqueous and organic solution, multibilay-

TABLE 2 IRfit analysis of spectra from labeled and unlabeled peptides in type CPM experiments

CPM-Unlabeled							
Frequency	1558.6	1582.7	1612.0	1628.0	1642.3	1659.0	1675.1
Width (FWHM)	42.3	32.9	21.2	20.1	26.3	32.0	20.0
Shape (% Gauss)	52.6	100.0	45.3	68.9	66.2	57.1	100.0
k	4 (3)	4 (2)	8 (1)	14 (2)	35 (3)	33 (3)	1 (1)
R_z	—	2.02 (0.50)	1.45 (0.12)	1.38 (0.17)	1.55 (0.03)	1.69 (0.07)	1.18 (1.00)
CPM-$CecA_{3-7}$							
Frequency	1575.9	1599.0	1609.6	1626.5	1642.6	1658.1	1674.1
Width (FWHM)	47.6	31.4	27.9	23.7	29.0	27.6	17.6
Shape (% Gauss)	68.5	69.6	28.8	72.1	100.0	100.0	83.0
k	11 (2)	3 (2)	14 (2)	13 (1)	37 (1)	18 (<1)	4 (<1)
R_z	1.29 (0.13)	—	1.21 (0.20)	1.57 (0.07)	1.61 (0.01)	1.94 (0.04)	2.05 (0.08)
CPM-$CecA_{26-30}$							
Frequency	1572.1	1599.5	1612.9	1628.4	1642.5	1657.4	1673.3
Width (FWHM)	35.1	36.2	25.5	21.7	25.8	28.0	18.9
Shape (% Gauss)	93.2	90.0	43.0	51.2	66.9	65.9	49.7
k	7 (<1)	11 (1)	8 (2)	14 (1)	32 (2)	23 (<1)	5 (1)
R_z	1.33 (0.52)	1.75 (0.78)	1.25 (0.45)	1.39 (0.51)	1.33 (0.45)	1.44 (0.53)	1.51 (0.57)

Spectra were fitted with IRfit over the frequency range 1700–1550 cm^{-1}. Total absorbance, *k*, is a percentage of total absorbance, and is calculated according to Eq. 4. The isotropic ratio (R_{ISO}) = 2.33 according to Eq. 4. Values of $R_Z > R_{ISO}$ indicate preferential orientation perpendicular to the membrane surface; values of $R_Z < R_{ISO}$ indicate preferential orientation parallel to the membrane. $R_Z = 0.84$ is the minimum possible dichroic ratio, corresponding to perfectly parallel orientation.
Values in parentheses represent the mean deviation of each result from an IRfit analysis of 18 spectra.

ers, single bilayers, high pressure monolayers, low pressure monolayers, and constant pressure monolayers. This information leads us to two principal conclusions. First, cecropin A folds while superficially adsorbed to a membrane, assuming a conformation that is distinct from that observed in aqueous solution. Second, it retains the same conformation and orientation after penetrating the membrane (Fig. 6). This indicates that the interactions responsible for folding the peptide are distinct and separable from those responsible for causing the folded peptide to penetrate the membrane and expand it against pressure.

The shape of its infrared spectrum suggests that the folded structure of cecropin A in monolayers and bilayers is similar to the structure determined in *d*-HFP/D_2O, i.e., a pair of helical segments connected and terminated by short random segments. However, the presence of spectral differences between these membrane preparations and *d*-HFP/D_2O (Fig. 3), the recovery of components at 1628 cm^{-1} and 1659 cm^{-1} by IRfit (Table 1), and the remarkably high degree of orientational order for residues 3–7 (Table 2), all suggest the presence of some β structure in the membrane-bound peptide. As noted in the figure captions, the spectral differences cannot be explained by the effects of anomalous dispersion. We cannot be more specific with this conformational analysis because the basis for making detailed secondary structure assignments to specific band components is, at best, only approximate.

We have concluded that the peptide does not make any direct contact with hydrophobic acyl chains of the membrane in HPM experiments because penetration of the peptide—even just the side chains—to this depth would necessitate membrane expansion, and this is not seen in HPM experiments. Preliminary data from low-angle x-ray reflectivity studies indicate that protegrins (another type of cationic antimicrobial peptide) do not penetrate into the choline layer when encountering a DPPC monolayer above its critical insertion pressure (K. Y. C. Lee, personal communication), and we suspect that cecropin A behaves similarly. Conversely, it is safe to conclude that cecropin A penetrates the membrane surface in SB_1 and SB_2 experiments because it causes membrane permeability changes in these vesicles (Silvestro et al., 1997).

We assume that membrane penetration to the level of the acyl chains also occurs in CPM experiments because changes in monolayer surface tension, without peptide penetration, would not yield a distinct critical insertion pressure. Furthermore, it is unlikely that superficially adsorbed peptides could expand a membrane without measurable consequences on acyl chain order. This is because the creation of new space between the acyl chains that is not occupied by peptide would necessitate tilting and thus disordering the acyl chains to fill this new space. Our data indicate that acyl chain order is quite high in CPM monolayer experiments whether or not peptide is present, whereas we can readily detect the disordering of acyl chains that accompanies peptide insertion in type SB_1 experiments (Silvestro and Axelsen, 1998). We see this disorder in SB_1 bilayer experiments (and not CPM monolayer experiments) most likely because interactions between the crystal surface and the bilayers prevents the bilayers from fully relaxing when the peptide inserts (the crystal surface is not present when peptide encounters membrane in CPM experiments).

We also assume that the spectra we collect in SB_1, SB_2, or CPM experiments arise from peptides that have penetrated the membrane, and not from superficially adsorbed peptide. Support for this assumption comes from our observation that peptide injection into the subphase expands the membrane in a CPM experiment, but that replacement of the subphase with peptide-free buffer does not reverse the expansion. This observation, combined with the very low affinity cecropin A exhibits for DMPC membranes (Silvestro et al., 1997), makes it likely that any superficially adsorbed peptide would diffuse off the membrane when the subphase is replaced with peptide-free buffer.

Finally, a tacit assumption of all attempts to characterize the membrane activity of a peptide is that the prevailing form of the peptide on the membrane is the same form that is responsible for its activity. The best evidence for this with

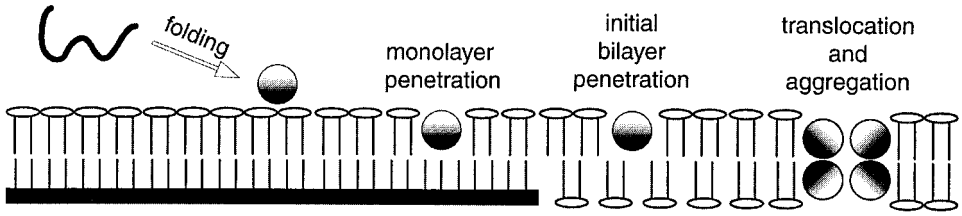

FIGURE 6 Proposed stages in the process of membrane recognition by cecropin A. The peptide is monomeric and unstructured in solution. Upon superficial adsorption to the membrane surface, it folds into a predominantly helical structure. The peptide helices are viewed end-on, with their hydrophilic aspects in white and their hydrophobic aspects in black. Peptide insertion into monolayers occurs without an increase in the disorder of monolayer acyl chains. Peptide insertion into the outer half of a preformed bilayer may induce some curvature in the membrane because this results in unequal expansion of the two halves of the bilayer. Bilayer membranes are closed surfaces, however, so that the ability of curvature to accommodate peptide in just one-half of the bilayer is limited. This likely leads to translocation of peptide to the inner half of the bilayer and the formation of aggregates with antimicrobial activity.

cecropin A is that vanishingly small amounts of peptide (on average, less than one molecule per vesicle) are able to permeabilize membranes in a significant fraction of a vesicle population (Silvestro et al., 1997). Although individual peptide molecules are probably not able to permeabilize membranes (Gazit et al., 1994), this indicates that the probability of any individual membrane-bound peptide being found in an active form at any given time appears to be reasonably high.

Membrane-induced folding

It is well known that lipid membranes tend to fold membrane-active peptides into various secondary structures (Kaiser and Kézdy, 1983, 1984, 1987; Schwyzer, 1995; White and Wimley, 1994, 1998). There are diverse forces operating in the vicinity of a membrane surface (Israelachvili, 1992), but little is known about which of them are specifically responsible for secondary structure formation and peptide folding. With the recent demonstration that magainin 2, like cecropin A, does not require anionic lipids to fold or exhibit permeabilizing membrane activity (Wieprecht et al., 1999), it seems likely that electrostatic forces between cationic antimicrobial peptides and anionic lipid headgroups will prove to be unimportant for the folding or activity of antimicrobial peptides in general.

It is noteworthy that the conformation and orientation of superficially adsorbed cecropin A does not change when it penetrates a membrane. The original "helical hairpin" hypothesis held that folding of helical peptides occurred before membrane penetration (Engelman and Steitz, 1981), and this is supported by experimental studies of transmembrane helical peptides (Hunt et al., 1997). Subsequent experimental (Jacobs and White, 1989) and theoretical (Milik and Skolnick, 1992, 1993) studies have suggested that helical peptides fold at the interface between hydrophilic and hydrophobic regions of a membrane before penetration. To apply this folding model to cecropin A, one must implicate a hydrophobic component on the membrane surface because cecropin A folds in HPM experiments where it cannot interact directly with the deeper and most hydrophobic regions of a lipid membrane. One possibility is the choline moiety of DMPC, which is polar, but unable to form hydrogen bonds. As the most superficial portion of a DMPC membrane, choline provides a relatively hydrophobic surface on which to fold a peptide.

Theoretical studies have suggested that merely reducing the number of degrees of freedom by association with an interface will increase the probability of secondary structure formation in polymer chains (Wattenbarger et al., 1990; Chan et al., 1991). It is pertinent to our results that polymer chains with weak forces drawing them to the interface were deemed more likely to form stable secondary structure in these studies than chains drawn by strong forces. This suggests that weak affinity between cecropin A and the choline moieties of DMPC may not only be sufficient to fold the peptide into an α-helix and orient it on the membrane surface, but weaker forces may even be more effective at this than stronger ones.

Once folded on the membrane surface, the ability of the peptide to expand the membrane against pressure indicates that there is a substantial energetic force driving peptide penetration. Presumably, this driving force is a consequence of favorable interactions between the folded peptide and the hydrophobic lipid acyl chains (Fig. 6). It has been suggested that peptide penetration may drive local bending of a membrane (Ludtke et al., 1996). However, membranes are closed surfaces and membrane curvature cannot accommodate an unlimited amount of peptide accumulation in the outer half of a bilayer. Thus, the need to equalize the areas of the inner and outer half-bilayers of a membrane may result in yet another force driving translocation of the peptide to the other half of the bilayer (as seen with melittin (Matsuzaki et al., 1997)). As long as the helical axes remain parallel to the membrane surface, as illustrated in Fig. 6, peptides in either half of the membrane would be indistinguishable by PATIR-FTIR spectroscopy.

Our data do not address whether cecropin A populates a superficially adsorbed and folded kinetic intermediate state before it penetrates a membrane, but this conclusion is supported by a recently published study of cecropin B interacting with phospholipid vesicles containing 25% anionic lipid (Wang et al., 1998). Using various stopped-flow techniques, a helical signal at 222 nm by CD was found to evolve with a single time constant of 1.3 s, whereas fluorescence intensity (from Trp_2) increased with two longer time constants, 2.2 and 5.7 s, and dye leakage from damaged vesicles increased with time constants of 2.0 and 9.6 s. These data are consistent with a three-stage temporal sequence involving 1) rapid and complete formation of secondary structure, 2) subsequent penetration of the membrane without refolding, and 3) reorganization to produce a transmembrane defect.

SUMMARY

The key finding of this study is that cecropin A folds and orients while superficially adsorbed to a membrane surface, and it remains in this configuration throughout all stages of its interaction with a membrane. Thus, the folding of cecropin A is driven by interactions with superficial components of the membrane, not deeper hydrophobic regions. Another separate set of interactions drives peptide penetration into these deeper regions. This result has broad implications for understanding how cecropin A exerts selective action against bacteria.

Our findings are derived from studies of cecropin A in chemically defined artificial membranes. It is abundantly clear that the behavior of this peptide differs between model membranes and the membranes of live bacteria (Silvestro et

al., 2000), just as it has long been known that its behavior differs between different bacterial species (Andreu et al., 1983). Nevertheless, its behavior on model membranes is inherently interesting, and is prerequisite to understanding its behavior in the vastly more complex chemical milieu of a bacterial membrane.

APPENDIX

The fractional contributions of different band components in a transmission spectrum are trivial to calculate, but not in polarized internal reflection spectra. Because the parallel and perpendicular-polarized spectra each represent only part of the total spectrum, they must be weighted according to the difference in electric field amplitudes for the two different polarizations to yield the correct total absorption. Assuming a uniaxial distribution about the z axis, the relationships between absorbance and electric field amplitudes are given by

$$A_x = \tfrac{1}{2} k\langle E_x^2\rangle\langle \sin^2\theta\rangle$$

$$A_y = \tfrac{1}{2} k\langle E_y^2\rangle\langle \sin^2\theta\rangle$$

$$A_z = k\langle E_z^2\rangle\langle \cos^2\theta\rangle$$

where θ is the angle between the transition moment and the z axis, and k is a proportionality factor incorporating both the extinction coefficient and the concentration of a substance.
Solving for k:

$$k = \frac{A_x}{\langle E_x^2\rangle} + \frac{A_y}{\langle E_y^2\rangle} + \frac{A_z}{\langle E_z^2\rangle}$$

Because:

$$A_\perp = A_y \quad \text{and} \quad A_\parallel = A_x + A_z$$

The measured absorbances $A_\parallel$ and $A_\perp$ relate to A_x, A_y, and A_z according to:

$$A_x = A_\perp \cdot \frac{\langle E_x^2\rangle}{\langle E_y^2\rangle}$$

$$A_z = A_\parallel - A_\perp \cdot \frac{\langle E_x^2\rangle}{\langle E_y^2\rangle}$$

Substitution yields an expression also derived by Marsh (1999):

$$k = \frac{A_\parallel}{\langle E_z^2\rangle} + \frac{A_\perp}{\langle E_y^2\rangle} \cdot \left(2 - \frac{\langle E_x^2\rangle}{\langle E_z^2\rangle}\right)$$

In practice, we use integrated areas (instead of $A_\parallel$ and $A_\perp$) for each component to calculate a value of k for each component. The fractional contribution of each band to the total band area is, therefore, the k value calculated for a given band component divided by the sum of k values calculated for all band components. Because the extinction coefficient applicable to any given band is not known, these calculations yield the contributions of each component to the total observed absorbance, not the fraction of molecules contributing to different elements of secondary structure.

The authors are grateful to J. D. Lear for the use of a ring tensiometer, and W. F. Degrado for the use of a mass spectrometer.

P.H.A. is supported by National Institutes of Health Grant GM54617 and a grant-in-aid from the American Heart Association.

REFERENCES

Adamson, A. W. 1990. Physical Chemistry of Surfaces. Wiley-Interscience, New York.

Andreu, D., R. B. Merrifield, H. Steiner, and H. G. Boman. 1983. Solid-phase synthesis of cecropin A and related peptides. *Proc. Natl. Acad. Sci. USA.* 80:6475–6479.

Andreu, D., R. B. Merrifield, H. Steiner, and H. G. Boman. 1985. N-terminal analogues of cecropin A: synthesis, antibacterial activity, and conformational properties. *Biochemistry.* 24:1683–1688.

Axelsen, P. H., W. D. Braddock, H. L. Brockman, C. M. Jones, R. A. Dluhy, B. K. Kaufman, and F. J. Puga II. 1995a. Use of internal reflectance infrared spectroscopy for the in-situ study of supported lipid monolayers. *Appl. Spectrosc.* 49:526–531.

Axelsen, P. H., and M. J. Citra. 1997. Orientational order determination by internal reflection infrared spectroscopy. *Prog. Biophys. Mol. Biol.* 66: 227–253.

Axelsen, P. H., B. K. Kaufman, R. N. McElhaney, and R. N. A. H. Lewis. 1995b. The infrared dichroism of transmembrane helical polypeptides. *Biophys. J.* 69:2770–2781.

Bartlett, G. R. 1959. Phosphorus assay in column chromatography. *J. Biol. Chem.* 234:466–468.

Brian, A. A., and H. M. McConnell. 1984. Allogeneic stimulation of cytotoxic T cells by supported planar membranes. *Proc. Natl. Acad. Sci. USA.* 81:6159–6163.

Chan, H. S., M. R. Wattenbarger, D. F. Evans, V. A. Bloomfield, and K. A. Dill. 1991. Enhanced structure in polymers at interfaces. *J. Chem. Phys.* 94:8542–8557.

Christensen, B., J. Fink, R. B. Merrifield, and D. Mauzerall. 1988. Channel-forming properties of cecropins and related model compounds incorporated into planar lipid membranes. *Proc. Natl. Acad. Sci. USA.* 85:5072–5076.

Citra, M. J., and P. H. Axelsen. 1996. Determination of molecular order in supported lipid membranes by internal reflection Fourier transform infrared spectroscopy. *Biophys. J.* 71:1796–1805.

Decatur, S. M., and J. Antonic. 1999. Isotope-edited infrared spectroscopy of helical peptides. *J. Am. Chem. Soc.* 121:11914–11915.

Engelman, D. M., and T. A. Steitz. 1981. The spontaneous insertion of proteins into and across membranes: the helical hairpin hypothesis. *Cell.* 23:411–422.

Gazit, E., A. Boman, H. G. Boman, and Y. Shai. 1995. Interaction of mammalian antibacterial cecropin P1 with phospholipid vesicles. *Biochemistry.* 34:11479–11488.

Gazit, E., W. J. Lee, P. T. Brey, and Y. Shai. 1994. Mode of action of the antibacterial cecropin B2—a spectrofluorometric study. *Biochemistry.* 33:10681–10692.

Glasoe, P. K., and F. A. Long. 1960. Use of glass electrodes to measure acidities in deuterium oxide. *J. Phys. Chem.* 64:188–190.

Goormaghtigh, E., V. Cabiaux, and J. M. Ruysschaert. 1994. Determination of soluble and membrane protein structure by Fourier-transform infrared spectroscopy. II. Experimental aspects, side chain structure, and H/D exchange. *Subcell. Biochem.* 23:363–403.

Hancock, R. E. W., and D. S. Chapple. 1999. Peptide antibiotics. *Antimicrob. Agents. Chemother.* 43:1317–1323.

Hoffmann, J. A. 1995. Innate immunity of insects. *Curr. Opin. Immunol.* 7:4–10.

Holak, T. A., A. Engstrom, P. J. Kraulis, G. Lindeberg, H. Bennich, T. A. Jones, A. M. Gronenborn, and G. M. Clore. 1988. The solution conformation of the antibacterial peptide cecropin A: a nuclear magnetic resonance and dynamical simulated annealing study. *Biochemistry.* 27: 7620–7629.

Huang, J. B., and M. W. Urban. 1992. Evaluation and analysis of attenuated total reflectance FT-IR spectra using Kramers-Kronig transforms. *Appl. Spectrosc.* 46:1666–1672.

Hunt, J. F., T. N. Earnest, O. Bousche, K. Kalghatgi, K. Reilly, C. Horvath, K. J. Rothschild, and D. M. Engelman. 1997. A biophysical study of integral membrane protein folding. *Biochemistry.* 36:15156–15176.

Israelachvili, J. N. 1992. Intermolecular and Surface Forces. Academic Press, San Diego.

Jacobs, R. E., and S. H. White. 1989. The nature of the hydrophobic binding of small peptides at the bilayer interface: implications for the insertion of transbilayer helices. *Biochemistry.* 28:3421–3437.

Kaiser, E. T., and F. J. Kézdy. 1983. Secondary structure of proteins and peptides in amphiphilic environments. *Proc. Natl. Acad. Sci. USA.* 80:1137–1143.

Kaiser, E. T., and F. J. Kézdy. 1984. Amphiphilic secondary structure: design of peptide hormones. *Science.* 223:249–255.

Kaiser, E. T., and F. J. Kézdy. 1987. Peptides with affinity for membranes. *Annu. Rev. Biophys. Biophys. Chem.* 16:561–581.

Kalb, E., S. Frey, and L. K. Tamm. 1992. Formation of supported planar bilayers by fusion of vesicles to supported phospholipid monolayers. *Biochim. Biophys. Acta.* 1103:307–316.

Ladokhin, A. S., and S. H. White. 1999. Folding of amphipathic alpha-helices on membranes: energetics of helix formation by melittin. *J. Mol. Biol.* 285:1363–1369.

Ludtke, S. J., K. He, W. T. Heller, T. A. Harroun, L. Yang, and H. W. Huang. 1996. Membrane pores induced by magainin. *Biochemistry.* 35:13723–13728.

Mancheno, J. M., M. Onaderra, A. Martinez del Pozo, P. Diaz-Achirica, D. Andreu, L. Rivas, and J. G. Gavilanes. 1996. Release of lipid vesicle contents by an antibacterial cecropin A-melittin hybrid peptide. *Biochemistry.* 35:9892–9899.

Marassi, F. M., S. J. Opella, P. Juvvadi, and R. B. Merrifield. 1999. Orientation of cecropin A helices in phospholipid bilayers determined by solid-state NMR spectroscopy. *Biophys. J.* 77:3152–3155.

Marsh, D. 1999. Quantitation of secondary structure in ATR infrared spectroscopy. *Biophys. J.* 77:2630–2637.

Matsuzaki, K., S. Yoneyama, and K. Miyajima. 1997. Pore formation and translocation of melittin. *Biophys. J.* 73:831–838.

Mchaourab, H. S., J. S. Hyde, and J. B. Feix. 1993. Aggregation state of spin-labeled cecropin AD in solution. *Biochemistry.* 32:11895–11902.

Mchaourab, H. S., J. S. Hyde, and J. B. Feix. 1994. Binding and state of aggregation of spin-labeled cecropin AD in phospholipid bilayers: effects of surface charge and fatty acyl chain length. *Biochemistry.* 33: 6691–6699.

Milik, M., and J. Skolnick. 1992. Spontaneous insertion of polypeptide chains into membranes: a Monte Carlo model. *Proc. Natl. Acad. Sci. USA.* 89:9391–9395.

Milik, M., and J. Skolnick. 1993. Insertion of peptide chains into lipid membranes: an off-lattice Monte Carlo dynamics model. *Proteins: Struct., Funct., Genet.* 15:10–25.

Momsen, W. E., J. M. Smaby, and H. L. Brockman. 1990. The suitability of nichrome for measurement of gas-liquid interfacial tension by the Wilhelmy method. *J. Colloid Interface Sci.* 135:547–552.

Ohta, K., and H. Ishida. 1988. Comparison among several numerical-integration methods for Kramers-Kronig Transformation. *Appl. Spectrosc.* 42:952–957.

Oren, Z., and Y. Shai. 1997. Selective lysis of bacteria but not mammalian cells by diastereomers of melittin: structure-function study. *Biochemistry.* 36:1826–1835.

Oren, Z., and Y. Shai. 1998. Mode of action of linear amphipathic alpha-helical antimicrobial peptides. *Biopolymers.* 47:451–463.

Pouny, Y., D. Rapaport, A. Mor, P. Nicolas, and Y. Shai. 1992. Interaction of antimicrobial dermaseptin and its fluorescently labeled analogues with phospholipid membranes. *Biochemistry.* 31:12416–12423.

Press, W. H., B. P. Flannery, S. A. Teukolsky, and W. T. Vetterling. 1986. Numerical Recipes. Cambridge University Press, Cambridge.

Schwyzer, R. 1995. In search of the "bio-active conformation"—is it induced by the target cell membrane? *J. Mol. Recognit.* 8:3–8.

Shai, Y. 1999. Mechanism of the binding, insertion and destabilization of phospholipid bilayer membranes by alpha-helical antimicrobial and cell non-selective membrane-lytic peptides. *Biochim. Biophys. Acta.* 1462: 55–70.

Silvestro, L., and P. H. Axelsen. 1998. Infrared spectroscopy of supported lipid monolayer, bilayer, and multibilayer membranes. *Chem. Phys. Lipids.* 96:69–80.

Silvestro, L., and P. H. Axelsen. 1999. FTIR linked analysis of conformational changes in annexin V upon membrane binding. *Biochemistry.* 38:113–121.

Silvestro, L., K. Gupta, J. N. Weiser, and P. H. Axelsen. 1997. The concentration-dependent membrane activity of cecropin A. *Biochemistry.* 36:11452–11460.

Silvestro, L., J. N. Weiser, and P. H. Axelsen. 2000. Antibacterial and antimembrane activities of cecropin A in *Escherichia coli. Antimicrob. Agents Chemother.* 44:602–607.

Steiner, H. 1982. Secondary structure of the cecropins: antibacterial peptides from the moth *Hyalophora cecropia. FEBS Lett.* 137:283–287.

Steiner, H., D. Andreu, and R. B. Merrifield. 1988. Binding and action of cecropin and cecropin analogues: antibacterial peptides from insects. *Biochim. Biophys. Acta.* 939:260–266.

Steiner, H., D. Hultmark, Å. Engström, H. Bennich, and H. G. Boman. 1981. Sequence and specificity of two antibacterial proteins involved in insect immunity. *Nature.* 292:246–248.

Tadesse, L., R. Nazarbaghi, and L. Walters. 1991. Isotopically enhanced infrared spectroscopy: a novel method for examining secondary structure at specific sites in conformationally heterogeneous peptides. *J. Am. Chem. Soc.* 113:7036–7037.

Urban, M. W. 1996. Attenuated Total Reflectance Spectroscopy of Polymers. American Chemical Society, Washington, D.C.

Wang, W., D. K. Smith, K. Moulding, and H. M. Chen. 1998. The dependence of membrane permeability by the antibacterial peptide cecropin B and its analogs, CB-1 and CB-3, on liposomes of different composition. *J. Biol. Chem.* 273:27438–27448.

Wattenbarger, M. R., H. S. Chan, D. F. Evans, V. A. Bloomfield, and K. A. Dill. 1990. Surface-induced enhancement of internal structure in polymers and proteins. *J. Chem. Phys.* 93:8343–8351.

White, S. H., and M. C. Wiener. 1995. Determination of the structure of fluid lipid bilayer membranes. *In* Permeability and Stability of Lipid Bilayers. E. A. Disalvo and S. A. Simon, editors. CRC Press, New York. 1–19.

White, S. H., and W. C. Wimley. 1994. Peptides in lipid bilayers: structural and thermodynamic basis for partitioning and folding. *Curr. Opin. Struct. Biol.* 4:79–86.

White, S. H., and W. C. Wimley. 1998. Hydrophobic interactions of peptides with membrane interfaces. *Biochim. Biophys. Acta.* 1376: 339–352.

Wiener, M. C., and S. H. White. 1992. Structure of a fluid dioleoylphosphatidylcholine bilayer determined by joint refinement of x-ray and neutron diffraction data. III. Complete structure. *Biophys. J.* 61: 434–447.

Wieprecht, T., M. Beyermann, and J. Seelig. 1999. Binding of antibacterial magainin peptides to electrically neutral membranes: thermodynamics and structure. *Biochemistry.* 38:10377–10387.

Wimley, W. C., K. Hristova, A. S. Ladokhin, L. Silvestro, P. H. Axelsen, and S. H. White. 1998. Folding of beta-sheet membrane proteins: a hydrophobic hexapeptide model. *J. Mol. Biol.* 277:1091–1110.

Yamamoto, K., and H. Ishida. 1994. Optical theory applied to infrared spectroscopy. *Vib. Spectrosc.* 8:1–36.